Mathematical Problems in Engineering
Volume 6, pp. 557–598
Reprints available directly from the publisher
Photocopying permitted by license only

Mixed H_2/H_∞ Control of Flexible Structures*

D. P. DE FARIAS, M. C. DE OLIVEIRA and J. C. GEROMEL†

LAC-DT/School of Electrical and Computer Engineering, UNICAMP, C.P. 6101, 13081-970, Campinas, SP, Brazil

(Received 18 January 2000)

This paper addresses the design of full order linear dynamic output feedback controllers for flexible structures. Unstructured H_∞ uncertainty models are introduced for systems in modal coordinates and in reduced order form. Then a controller is designed in order to minimize a given H_2 performance function while keeping the maximum supported H_∞ perturbation below some appropriate level. To solve this problem we develop an algorithm able to provide local optimal solutions to optimization problems with convex constraints and non-convex but differentiable objective functions. A controller design procedure based on a trade-off curve is proposed and a simple example is solved, providing a comparison between the proposed method and the usual minimization of an upper bound to the H_2 norm. The method is applied to two different flexible structure theoretical models and the properties of the resulting controllers are shown in several simulations.

Keywords: Flexible structures; Mixed H_2/H_∞ control; Numerical methods

1. INTRODUCTION

The control of flexible structures poses several challenges that may be very difficult to handle by standard synthesis procedures. The dynamics of such systems are usually high order and present many closely spaced low frequency modes. Finite-element methods which are the usual source of mathematical models of real world flexible

* This work has been supported in part by grants from "Fundação de Amparo à Pesquisa do Estado de São Paulo – FAPESP" and "Conselho Nacional de Desenvolvimento Científico e Tecnológico – CNPq", Brazil.

† Corresponding author. e-mail: geromel@dt.fee.unicamp.br

structures are known to provide models which may not accurately describe high order modes dynamics. Theoretical flexible structure models are infinite dimensional and must be preprocessed by some truncation or order reduction procedure before being used in controller design. All such features ask for the introduction of some kind of uncertainty modeling in the design process so that the obtained controllers may succeed when applied to the real physical structure. Furthermore, in view of the high order of the plant dynamics the controller must be able to handle only a reduced set of measurements, which in practice discards the use of a state feedback structure.

The most powerful procedures available in the literature to the design of controllers for uncertain systems are based either on H_∞ or quadratic stability theory. The very particular form of flexible structure models leads in general to a highly structured uncertainty description. In this context, due to its inherent ability to deal with structured uncertainty, the quadratic stability approach would be much more advantageous than an H_∞ one. However, despite the effort of many authors (see for instance [1, 2]), no necessary and sufficient condition for quadratic stabilizability under output feedback is available.

On the other hand, several results are known to handle the H_∞ controller design under output feedback [3], although most available procedures are fit to deal with unstructured uncertainty, which may turn the design very conservative. Despite this fact, many authors (see for instance [4, 5]) have been successful in providing uncertainty models that worked well in an unstructured H_∞ design framework. With respect to performance, this unstructured framework does not easily admit the introduction of additional H_∞ performance constraints without increasing conservativeness, which generally asks for some compromise solution. Some authors try to reduce conservativeness with a H_∞/μ synthesis approach [6].

In order to try to overcome some of these difficulties we propose to address this problem on a mixed H_2/H_∞ framework. The approach involves three steps: (a) setup of an H_∞ unstructured uncertainty model to cope with plant uncertainty, (b) numerical solution to a mixed control problem whose objective is the minimization of an H_2 performance cost subject to the H_∞ constraint developed in Step (a), and (c) development of a controller design procedure.

The first step, the H_∞ unstructured model, is developed with the introduction of a variational model around a given nominal plant in modal coordinates. The same idea is extended to cope with reduced order models. The second step, the solution to the mixed H_2/H_∞ problem, is done by a numerical algorithm that is able to find a local optimal solution to the mixed problem with respect to a six port generalized plant. A controller parametrization is chosen such that the set of controllers satisfying the H_∞ constraint is given by a convex set while the minimization is performed with respect to the actual H_2 norm rather than some upper bound. The third step, the controller design procedure, is based on the derivation of a strategy that provides a trade-off curve with which the designer may choose the controller that satisfies the compromise between robustness (in the H_∞ sense) and performance (in the H_2 sense).

This design procedure is tested on two theoretical flexible structure models and the performance of the obtained controllers is verified by several simulations.

The notation used in the paper is standard. Upper-case italic letters denote matrices while lower-case italic letters denote vectors. For a matrix X, X' is the transpose of X and X^{-1} is the inverse of X. The notation $X > 0$ means that X is a symmetric and positive definite real matrix and trace $[X]$ denotes its trace.

2. ROBUST H_∞ DESIGN

Flexible structure models are usually given in the form

$$\ddot{x} + \Gamma\dot{x} + \Lambda x = Bu \tag{1}$$

$$y = Ex + F\dot{x} \tag{2}$$

where $B \in R^{n \times m}$, $E, F \in R^{r \times n}$, Γ and Λ are diagonal $n \times n$ matrices with entries

$$\Gamma_{i,i} = 2\xi_i\omega_i \tag{3}$$

$$\Lambda_{i,i} = \omega_i^2 \tag{4}$$

In this form $x \in R^n$ is known as the modal coordinates. Many times flexible structure theoretical and finite-element models are developed

such that matrix $\Gamma = 0$, *i.e.*, they are undamped, and damping is added to the system a *posteriori* with the introduction of the damping factors ξ_i. This system can be represented by the state space equations

$$\dot{x} = A_n x + B_n u \tag{5}$$

$$y = C_n x \tag{6}$$

where

$$A_n = \begin{bmatrix} 0 & I \\ -\Lambda & -\Gamma \end{bmatrix}, \quad B_n \begin{bmatrix} 0 \\ B \end{bmatrix}, \quad C_n = [E \quad F]$$

In [4] a left-coprime factorization is applied to the Laplace transform of the system in (1), (2) and a structured perturbation model is developed from the real parametric uncertainty bounds along with a particular weighting function. Although the nature of the perturbation model is taken to be highly structured the actual design is performed as if the perturbation were really unstructured, by finding a standard full-order output feedback controller that satisfies a γ level constraint in the closed-loop H_∞ norm. Of course, provided there exists a feasible solution to this *relaxed* problem, the obtained controller will drive the system with some degree of conservativeness. As stated in the introduction, if compared with available structured uncertainty design methods, this approach has a much simpler computational solution and that is the reason why it is accepted.

However, a strange situation may occur if there exists no feasible controller which satisfies the unstructured design requirements. In this case, one usual procedure is trying to find a *less robust* controller relaxing the γ level of the H_∞ constraint in the hope that the inherent degree of conservativeness of the solution still provides a controller which happens to be robust in face of the original structured uncertainty level. It is clear that there are no guarantees that this will happen and in many instances this procedure will simply not work.

In view of this fact, it is desirable that the control engineer be able to modify the unstructured design requirements (and not only the γ level) in order to try to obtain a controller that will be useful for the original structured problem. In the formulation of [4] that could be done, for instance, by carefully tuning the weighting function, which does not seem to be an easy task. Furthermore, possible changes in the order of

the weighting function may contribute to increase even more the order of the full design problem and, consequently, of the obtained controller.

In order to overcome this difficulties we introduce a normalized variational uncertainty model which is much simpler and naive than the model described in [4] but which provides enough room for the control engineer to change some of the available parameters in order to adequately tune a controller. In this model the uncertainty description is less realistic, in the sense that it is not directly drawn from bounds in the real parameter range of variations, but is much simpler and, since it does not deal with frequency dependent scalings or weighting functions, it may be changed without increasing the order of the generalized plant. The basic idea is to induce in the state space models (5), (6) unstructured matrix perturbations in the form

$$A(\Delta) = \begin{bmatrix} 0 & I \\ -(I+\Delta_1)\Lambda & -(I+\Delta_1)\Gamma \end{bmatrix}, \tag{7}$$

$$B(\Delta) = \begin{bmatrix} 0 \\ (I+\alpha\Delta_2)B \end{bmatrix}, \quad C(\Delta) = [E(I+\alpha\Delta_3) \quad F(I+\alpha\Delta_3)] \tag{8}$$

which can be represented by the usual four port model

$$\dot{x} = Ax + B_1 w_1 + B_2 u \tag{9}$$

$$y = C_2 x + D_{21} w \tag{10}$$

$$z_1 = C_1 x + D_{12} u \tag{11}$$

with

$$B_1 = \begin{bmatrix} 0 & 0 & 0 \\ I & I & 0 \end{bmatrix}, \quad C_1 = \begin{bmatrix} -\Lambda & -\Gamma \\ 0 & 0 \\ I & 0 \\ 0 & I \end{bmatrix},$$

$$D_{12} = \alpha \begin{bmatrix} 0 \\ B \\ 0 \\ 0 \end{bmatrix}, \quad D_{21} = \alpha \begin{bmatrix} 0 & 0 \\ 0 & 0 \\ E & F \end{bmatrix}$$

So, we can ensure that if the H_∞ norm of the closed-loop transfer function from w_1 to z_1 is less than γ, then the system is robust to unstructured perturbations in the form

$$w_1 = \Delta z_1, \quad \|\Delta\|_\infty < \gamma^{-1}$$

In this case it is also immediate to conclude that (7), (8) is robustly stable since the following structured perturbations are such that

$$\Delta = \text{block diag } \{\Delta_1, \alpha\Delta_2, \alpha\Delta_3\}, \quad \|\Delta_i\|_\infty < \gamma^{-1}, \quad i = 1,2,3$$

Notice that doing so we are also designing with the help of an unstructured perturbation *version* of the desired structured model. It is important to remark that, on the contrary of [4], we consider perturbations on both B_n and C_n matrices. Also notice the role of the scalar parameter α, which scales matrices Δ_2 and Δ_3. It is easy to see that the resulting robust design will be such that

$$\|\Delta_i\|_\infty < (\alpha\gamma)^{-1}, \quad i = 2,3$$

so that setting $\alpha > 1$ we may lower the requirement of robustness face to uncertainties in the input and output matrices without changing the importance of robustness face to the dynamic uncertainty matrix Δ_1. As it will be seen in the experiments, this parameter will be very useful in achieving feasible designs. Also notice that in the form it was introduced (multiplying both matrices D_{12} and D_{21}) it also works reducing the influence of the term $D_{12}\Delta D_{21}$ in the final design, which appears multiplied by the square of α. Note that this term only becomes significant because we have to consider in the synthesis procedure the disturbances as being unstructured.

Finally, it is very easy to weigh the influence of the uncertain matrices Δ_i, $i = 1,2,3$ in the obtained controller with the introduction of multiplier matrices in B_1 and C_1. For instance, one is allowed to redefine

$$B_1 = \begin{bmatrix} 0 & 0 & 0 \\ S_1 & S_2 & 0 \end{bmatrix}, \quad C_1 = \begin{bmatrix} -\Lambda & -\Gamma \\ 0 & 0 \\ S_3 & 0 \\ 0 & S_4 \end{bmatrix}$$

such that the resultant uncertainty model becomes

$$A(\Delta) = \begin{bmatrix} 0 & I \\ -(I + S_1\Delta_1)\Lambda & -(I + S_1\Delta_1)\Gamma \end{bmatrix},$$

$$B(\Delta) = \begin{bmatrix} 0 \\ (I + \alpha S_2\Delta_2)B \end{bmatrix},$$

$$C(\Delta) = [E(I + \alpha\Delta_3 S_3) \quad F(I + \alpha\Delta_3 S_4)]$$

By carefully defining these scaling matrices we can actively change the unstructured uncertainty model in order to achieve a desired robust performance. For instance, defining the scaling matrix S_1 as a positive diagonal matrix we may increase or decrease the importance of considering uncertainty in selected modes. In this form, *a priori* knowledge about bounds of the real system parameters can be taken into account by the design procedure.

An important point is that this uncertainty model does not require any frequency dependent weighting function, which means that the order of the generalized plant is the same as that of the original plant, and so is the order of the obtained controller.

Another drawback of the design based on structured uncertainty bounds is that it may be difficult to *convert* these bounds if the order of the state space model is to be reduced by some order reduction procedure. This happens since standard order reduction procedures, like balanced truncation [7, 8], destroy the diagonal structure in (1), (2). On the other hand, a reduced order normalized variational uncertainty model is immediately available. For instance, it is possible to extend the considerations above to the following uncertainty model

$$\begin{gathered} A_r(\Delta) = (I + \Delta_1)A_{nr}, \quad B_r(\Delta) = (I + \alpha\Delta_2)B_{rn}, \\ C_r(\Delta) = C_{rn}(I + \alpha\Delta_3) \end{gathered} \tag{12}$$

where the matrices subscripted by r are obtained from the models (1), (2) by some order reduction procedure.

3. H_2 PERFORMANCE AND THE MIXED H_2/H_∞ CONTROL PROBLEM

In the analysis of flexible structures the time response to an impulsive input is of great value in the comprehension of the system behavior, and it is natural to consider as the closed loop performance index to be minimized in the controller synthesis the H_2 norm of the closed loop transfer function [9]. More specifically, denoting by $T(z, w; s)$ the transfer function from the input w to the output z and with respect to the six port generalized plant

$$\dot{x} = Ax + B_0 w_0 + B_1 w_1 + B_2 u \tag{13}$$

$$y = C_2 x + D_{20} w_0 + D_{21} w_1 \tag{14}$$

$$z_0 = C_0 x + D_0 u \tag{15}$$

$$z_1 = C_1 x + D_{12} u \tag{16}$$

our objective is to design a controller that minimizes the H_2 norm of the closed loop transfer function from w_0 to z_0 and keeps the H_∞ norm of the transfer function from w_1 to z_1 under some prescribed level, *i.e.*, to find a solution to the mixed H_2/H_∞ control problem

$$\min\{\|T(z_0, w_0; s)\|_2 : \|T(z_1, w_1; s)\|_\infty < \gamma\} \tag{17}$$

From the discussion in the previous section, by choosing the value of γ we control the trade-off between robustness and performance of the design. In this sense the larger γ, the easier it will be to satisfy the mixed problem constraint; nonetheless, this will be accomplished at the expense of reducing the acceptable level of perturbation to which the system will remain stable.

4. NUMERICAL SOLUTION TO THE MIXED H_2/H_∞ CONTROL PROBLEM

Until today, there is no numerical algorithm in the literature that can find an optimal solution (not even a local one) to the control problem stated in the previous section. Both state and dynamic output feedback

control problems remain unsolved. Imposing extra assumptions, for instance $w = w_0 = w_1$, some existing methods are able to find a sub-optimal solution based on the minimization of an upper bound to the objective function. This procedure, as illustrated in [3], may produce poor solutions, which do not present a sound decrease in $\| T(z_0, w_0; s) \|_2$.

In this section we propose a numerical algorithm that is able to find a local optimal solution to the mixed H_2/H_∞ problem without any additional assumption. The algorithm, generically described below, may also be applied to other optimization problems formulated in the same form.

The main point is the following. Applying suitable changes of variables, it is possible to rewrite the mixed H_2/H_∞ problem (17) in the form

$$\min_x \{ f(x) : x \in \mathcal{X} \} \tag{18}$$

where $f(\cdot)$ is a non-convex yet differentiable function and $\mathcal{X}$ is a convex set.

4.1. A Conceptual Algorithm

In the following, the convex set $\mathcal{X}$ will always be considered as described by an LMI (Linear Matrix Inequality), that is,

$$\mathcal{X} = \left\{ x | F(x) := F_0 + \sum_{i=1}^{N} F_i x_i > 0 \right\}$$

where all matrices F_i, $i = 1, \ldots, N$ are real, square and symmetric. Furthermore, we assume that x_k is a feasible point, *i.e.*, $F(x_k) > 0$, and define the following convex optimization problem

$$\min_z \{ \langle \nabla f(x_k), z \rangle : F(z) > 0 \} \tag{19}$$

Let z_k be its optimal solution and, keeping in mind that x_k is a feasible solution,

$$\langle \nabla f(x_k), z_k - x_k \rangle \leq 0$$

Therefore, defining $d_k := z_k - x_k$, two different situations are possible:

(1) $\langle \nabla f(x_k),\ d_k \rangle < 0$. In this case, since the constraint set is convex, the point

$$x_{k+1} = x_k + \alpha d_k$$

will always be feasible for $0 \leq \alpha \leq 1$. Furthermore, if we expand $f(\cdot)$ in Taylor series, we obtain

$$f(x_{k+1}) = f(x_k) + \alpha \langle \nabla f(x_k), d_k \rangle + \mathcal{O}(\alpha^2)$$

which makes clear that there is an $\alpha > 0$ small enough so that $f(x_{k+1}) < f(x_k)$. Thus, by performing an unidimensional search through the direction d_k we may simultaneously decrease the objective function and find a new feasible point.

(2) $\langle \nabla f(x_k),\ d_k \rangle = 0$. In this case, with no loss of generality, we can consider $z_k = x_k$. Hence, the necessary and sufficient optimality conditions for the problem (19) can be written as

$$\begin{aligned} \langle Z, F(x_k) \rangle &= 0 \\ \nabla f(x_k)_i - \langle Z, F_i \rangle &= 0 \\ F(x_k) > 0, \quad Z = Z' &\geq 0 \end{aligned}$$

One should notice that these are indeed the necessary optimality conditions for problem (18), which implies that x_k is also a local optimal to the mixed problem.

It follows that the following numerical method converges to a local optimal solution to the problem (18) (see [10]). The only hypothesis which must be adopted is that there exists an initial feasible point x_0, which is equivalent to assuming that there exists a controller such that the H_∞ norm of the closed-loop transfer function from w_0 to z_0 is less than the given $\gamma > 0$. Naturally, if there is no controller with this property the mixed problem has no feasible solution. So, the following algorithm can be stated:

(1) Let x_0 be any point such that $F(x_0) > 0$. If there is no such x_0, problem (18) has no solution. Set the iteration counter $k = 0$.

(2) Solve the following convex optimization problem

$$z_k := \arg \min_z \{ \langle \nabla f(x_k), z \rangle : F(z) > 0 \}$$

Let $d_k := z_k - x_k$ and $\theta_k := \langle \nabla f(x_k),\ d_k \rangle$.

(3) According to a prespecified precision, if $\theta_k \approx 0$, x_k is a local optimal solution, then stop. Otherwise go to Step 4.
(4) Solve the unidimensional search problem

$$\alpha_k := \arg \min_{\alpha} \{ f(x_k + \alpha d_k) : 0 \leq \alpha \leq 1 \}$$

Let $x_{k+1} := x_k + \alpha_k d_k$, $k \leftarrow k+1$ and go to Step 2.

This algorithm generates a decreasing sequence $f(x_{k+1}) \leq f(x_k)$ which converges to a local optimal solution.

4.2. Comments and Acceleration

The main computational work in the above algorithm is concentrated in Steps 2 and 4. The unidimensional search (Step 4) depends exclusively on the shape of the nonconvex function $f(\cdot)$ and thus, any possible acceleration strategy should explore particular properties of this function. On the other hand, Step 2 is the solution of a linear objective optimization problem subject to LMI constraints, which may be efficiently solved by many available interior-point methods. Nonetheless, a closer look at this step may suggest the introduction of some *acceleration* techniques.

In order to solve the problem in Step 2, primal interior point methods (see [11]) may internally generate a sequence of approximate minimizers to the convex penalized function

$$g(z) = \langle \nabla f(x_k), z \rangle + \beta b(z)$$

where $b(z)$ is a barrier function associated with the constraints. For instance, take $b(z)$ as the usual convex logarithmic barrier

$$b(z) = -\log \det[F(z)]$$

Starting from a feasible approximate minimizer this sequence is generated reducing the value of β then performing Newton steps until another approximate minimizer associated to each decreasing value of β is available. At each Newton step an unidimensional search is performed in the direction

$$d_N := d_f + \beta d_b = -H^{-1}(z)(\nabla f(x_k) + \beta \nabla b(z))$$

where $H(z)$ is the Hessian matrix of $g(z)$ which obviously coincides with the Hessian matrix of $b(z)$. From the convexity of $b(z)$ matrix $H(z)$ is positive definite, which implies that performing an unidimensional search over d_N the cost will indeed decrease (d_N is a descent direction) as long as $\beta > 0$. For us, it is interesting to notice what happens when β tends to 0, in which case $d_N \to d_f$. In this case, roughly speaking, the influence of the barrier function in the optimization direction is kept at the minimum possible level, acting only in order to deviate this direction when it is too close to the boundary of the convex set.

Therefore, we may simply impose $\beta \to 0$ at each iteration such that in only one step a new feasible point z_k with all desired properties (smaller cost and feasibility) is produced. Doing this we are able to introduce new information about the function $f(\cdot)$, the actual objective function to be minimized, at each iteration. Hence the determination of d_k in Step 2 may be replaced by the determination of

$$d_k = -H(x_k)^{-1} \nabla f(x_k)$$

It should also be noticed that the largest possible value of α, for which $x_k + \alpha d_k$ is still feasible, is given as [12]

$$\alpha_{\max} = 1/\lambda_{\max}\left[F(x_k)^{-(1/2)}(F(d_k) - F(0))F(x_k)^{-(1/2)}\right]$$

and therefore the unidimensional search of Step 4 should be altered to reflect the feasibility interval $0 \leq \alpha < \alpha_{\max}$. In the linear case this method is known as the *affine scaling algorithm*. It is interesting to notice that setting $H(x_k) = I$ the algorithm becomes a pure steepest-descent algorithm and, since the constraints are not taken into account when choosing the descent direction, d_k reduces to the gradient of the unconstrained problem.

Our experience with all versions of these algorithms shows that replacement of d_k by the affine scaling direction is effective in providing a significant reduction in the computational work required to find a local optimal and generally does not alter the optimality degree of the obtained solution when compared with the original Step 2. Furthermore, every time the algorithm stops in a local optimum we can try reinitialize it by performing one step in the form of the original

Step 2 which in some cases will provide a direction through which the cost function can be even more decreased.

4.3. Solving the Mixed H_2/H_∞ Control Problem

In order to be solved by the algorithm introduced above it is necessary to rewrite the mixed H_2/H_∞ control problem (17) in a suitable form. In order not to obfuscate the reader with the algebraic complexity of the formulae that arises in the output feedback case, we will introduce the basic procedures with respect to a much simpler problem, the state feedback control problem. Besides adding to the completeness of this paper, state feedback results will be used by one of the possible output feedback parametrizations to be introduced.

4.3.1. State Feedback

In the state feedback problem we assume the whole state vector is being measured. With respect to the plants (13)–(16) we turn our attention to the determination of the linear feedback law

$$u = Kx$$

which solves the mixed H_2/H_∞ problem.

By performing the change of variables $K = LX^{-1}$, with $X = X'$, we may state that [3]

$$\|T(z_1, w_1; s)\|_\infty < \gamma \Longleftrightarrow (L, X) \in \mathcal{X}$$

where $\mathcal{X}$ is the convex set defined by all pairs (L, X) such that

$$\begin{bmatrix} AX + XA' + B_2L + L'B_2' + B_1B_1' & (\cdot)' \\ C_1X + D_{12}L & -\gamma^2 I \end{bmatrix} < 0, \quad X > 0$$

Notice that this set is an LMI. Furthermore, since every gain K corresponding to a pair $(L, X) \in \mathcal{X}$ stabilizes the system under consideration, through the substitution of K it follows that the norm $\|T(z_0, w_0; s)\|_2^2$ may be expressed as a function of L and X, namely [3],

$$f(L, X) = \operatorname{trace}\left[(C_0 + D_0LX^{-1})P(C_0 + D_0LX^{-1})'\right] \tag{20}$$

where trace[·] denotes the trace of (·) and

$$P = \int_0^\infty e^{(A+B_2LX^{-1})t} B_0 B_0' e^{(A+B_2LX^{-1})'t} dt$$

is the closed loop controlability grammian. In this way, the mixed H_2/H_∞ state feedback problem can be rewritten in the form

$$\min_{L,X} \{ f(L,X) : (L,X) \in \mathcal{X} \}$$

where $\mathcal{X}$ is a convex set expressed by LMI, being thus solved by the proposed algorithm. The only open question concerns the calculation of the gradient of $f(X, L)$, which can be found in Appendix A.

4.3.2. Output Feedback

Returning to the output feedback problem with respect to the generalized plant (13)–(16) we shall consider the following dynamic output feedback controllers with the same order as that of the given plant

$$\dot{x}_c = A_c x_c + B_c y \tag{21}$$

$$u = C_c x_c \tag{22}$$

and, with no loss of generality [3], we impose $D_{12}' D_{12} = I$ and $D_{21} D_{21}' = I$.

For the output feedback problem we devise two possible approaches that reduce the control problem to the form (18), being thus solvable by the algorithm previously proposed. The first of them which we describe in the sequel makes use of the well known observer based parametrization. So, given the following particular controller structure

$$A_c = A_\infty + B_{2\infty} K + L_\infty C_2, \quad B_c = -L_\infty, \quad C_c = K \tag{23}$$

where

$$A_\infty = A + \gamma^{-2} \Pi_\infty C_1' C_1, \quad B_{2\infty} = B_2 + \gamma^{-2} \Pi_\infty C_1' D_{12},$$
$$L_\infty = -\Pi_\infty C_2' - B_1 D_{21}'$$

and Π_∞ is the stabilizing semidefinite positive solution to the Riccati equation

$$\Pi A_f' + A_f \Pi - \Pi(C_2' C_2 - \gamma^{-2} C_1' C_1)\Pi + B_{1f} B_{1f}' = 0$$

with

$$A_f = A - B_1 D_{21}' C_2, \quad B_{1f} = B_1(I - D_{21}' D_{21})$$

the following are equivalent

(a) $\| T(z_1, w_1; s) \|_\infty < \gamma$

(b) With respect to the auxiliary system

$$\mathcal{G}: \begin{cases} \dot{x} = A_\infty x + L_\infty w_1 + B_{2\infty} u \\ z_1 = C_1 x + D_{12} u \\ u = Kx \end{cases}$$

there exists a state feedback gain K such that $\|T_{\mathcal{G}}(z_1, w_1; s)\|_\infty < \gamma$.

(c) There exists (X, L) such that the LMI

$$\begin{bmatrix} A_\infty X + X A_\infty' + B_{2\infty} L + L' B_{2\infty}' + L_\infty L_\infty' & (\cdot)' \\ C_1 X + D_{12} L & -\gamma^2 I \end{bmatrix} < 0, \quad X > 0 \qquad (24)$$

is feasible and $K = LX^{-1}$.

For a proof of equivalence between items (a) and (b) see [3]. Item (c) is a consequence of the state feedback parametrization that we have just discussed.

In this way, considering $\mathcal{X}$ as the linear inequality (24) and performing the change of variables $K = LX^{-1}$ in the controller structure (23), as in the state feedback case, it is possible to calculate the function $f(X, L) = \|T(z_0, w_0; s\|_2^2$ in terms of the closed loop observability grammian and rewrite the observer based output feedback control problem in the form

$$\min_{L,X} \{ f(L, X) : (L, X) \in \mathcal{X} \}$$

as desired.

It is important to emphasize some aspects of the solution we are proposing here. First of all, although the convex set (24) is equivalent to an H_∞ constraint defined with respect to the auxiliary state feedback plant $\mathcal{G}$, the H_2 norm minimization is performed with respect to the closed loop H_2 norm of $T(z_0, w_0; s)$ of the original system rather than that of $\mathcal{G}$. In this second case, although the gradient calculations are greatly simplified, it may be shown that the obtained solution is very conservative since we are implicitly assuming that the closed loop observability grammian is constrained to present a very particular structure.

Also notice that under the additional assumption $w = w_0 = w_1$ a suboptimal solution is available once it is possible to show that [3, 13]

$$\|T(z_0, w_0; s)\|_2^2 \leq \text{trace}[C_0 \Pi_\infty C_0'] + \text{trace}[(C_0 + D_0 K) X (C_0 + D_0 K)']$$

As we will see in the numerical experiments, considering the minimization of this upper bound instead of the actual H_2 norm may lead to a very poor solution, specially for low values of γ. Of course, the main advantage of this approach is that the change of variables introduced above is able to render the whole problem convex.

The second possible approach to the mixed H_2/H_∞ output feedback problem is the use of the general output feedback controller parametrization as described, for instance, in [14, 1]. In this case, all controller matrices A_c, B_c and C_c must be determined by optimization procedures.

As it is shown in [14], the constraint $\|T(z_1, w_1; s)\|_\infty < \gamma$ is equivalent to the LMI constraints

$$\begin{bmatrix} A'Y + Y_A + FC_2 + C_2'F' + \gamma^2 C_1' C_1 & (\cdot)' \\ B_1'Y + D_{21}'F' & I \end{bmatrix} < 0 \tag{25}$$

$$\begin{bmatrix} AX + XA' + B_2 L + L'B_2' + B_1 B_1' & (\cdot)' \\ C_1 X + D_{12} L & -\gamma^2 I \end{bmatrix} < 0 \tag{26}$$

$$\begin{bmatrix} X & I \\ I & Y \end{bmatrix} > 0 \tag{27}$$

Furthermore, for every feasible matrices (L, X, F, Y) the corresponding controller can be calculated by the following steps [1]:

(1) Calculate

$$M = -A - XA'Y - L'B_2'Y - XC_2'F' - B_1(B_1'Y + D_{21}'F') - \gamma^{-2}(XC_1' + L'D_{12}')C_1$$

(2) Choose a non-singular V and let $B_c = V^{-1}F$;
(3) Calculate[1] $U = (I - XY)(V')^{-1}$ and set $C_c = L(U')^{-1}$;
(4) Set $A_c = V^{-1}M'(U')^{-1}$.

Some considerations about the choice of U and V should be made. It is not difficult to see that the choices given above reduce the controller transfer function to

$$C(s) = C_c(sI - A_c)^{-1}B_c = F[s(I - YX) - M']L$$

which does not depend on U and V. Those variables, however, define a particular state space representation for the controller with, obviously, the same transfer function.

So, setting the LMI (25)–(27) as the convex set $\mathcal{X}$, it is clear that

$$\|T(z_1, w_1; s)\|_\infty < \gamma \Longleftrightarrow (L, X, F, Y) \in \mathcal{X}$$

Finally, for any nonsingular choice of matrix V and the corresponding matrix $U(X, Y, V)$, we are able to obtain a function $f(L, X, F, Y) = \|T(z_0, w_0; s)\|_2^2$ such that output feedback mixed H_2/H_∞ problem with a general controller can be written as

$$\min_{L,X,F,Y} \{f(L, X, F, Y) : (L, X, F, Y) \in \mathcal{X}\}$$

As a final remark, although theoretically speaking any choice of matrix U and V is possible, one should be aware that with regards to the numerical implementations of the unidimensional search and gradient calculations some particular choices may lead to significant simplifications.

[1] Notice that U is invertible since $Y > X^{-1}$.

5. CONTROLLER DESIGN PROCEDURE

With the tools developed in the previous sections we are able to develop a mixed H_2/H_∞ controller design procedure that will be used in the experiments presented in this paper. In this setup, we wish to provide the designer with the ability to select a controller that represents an adequate compromise between robustness and performance. So, with respect to the plants (13)–(16) we start determining the minimum possible value of the closed loop H_∞ norm of the transfer function from w_1 to z_1

$$\gamma_{\min} = \min \|T(z_1, w_1; s)\|_\infty$$

Notice that regardless of the output feedback controller parametrizations introduced in the last section we will always be able to find the same minimum value for $\gamma_{\min}$. Now, starting with a value of $\gamma = \gamma_0$ slightly above $\gamma_{\min}$ we find a feasible initial controller, run the algorithm of Section 4 and get a local optimal solution to the mixed H_2/H_∞ control problem for any chosen controller parametrization. Notice that if the value of γ_0 is sufficiently close to $\gamma_{\min}$ the norm of the obtained mixed controller will be approximately the H_2 norm of $T(z_0, w_0; s)$ calculated with the minimal H_∞ controller. Now, setting $k = 1$ and observing that the algorithm in Section 4 always provides a local optimal solution to the mixed H_2/H_∞ problem we relax the value of $\gamma_k > \gamma_{k-1}$ and run the algorithm taking as a feasible initial solution the optimal solution associated to γ_{k-1}. In this way we may ensure that the following property will always hold

$$\|T(z_0, w_0; s, \gamma_k)\|_2 \leq \|T(z_0, w_0; s, \gamma_{k-1})\|_2$$

where the dependency of γ is to emphasize that these norms are evaluated for the optimal controllers obtained as explained. In this manner we are able to draw a trade-off curve between robustness (measured by the H_∞ norm) and performance (measured by the H_2 norm) and adequately select a controller that satisfies the project specifications. A summary of this design procedure is given below:

(1) Determine the minimal H_∞ closed loop norm $\gamma_{\min}$.
(2) Set $\gamma_0 = (1+\varepsilon)\gamma_{\min}$, $\varepsilon > 0$, and determine a local optimal solution to the mixed H_2/H_∞ control problem. Set $k = 1$.

(3) Starting from the mixed H_2/H_∞ local optimal solution associated to the value of γ_{k-1}, set $\gamma_k > \gamma_{k-1}$ and apply the algorithm in Section 4 to determine the current local optimal solution.

(4) If $\gamma_k \geq \gamma_{\max}$, $\gamma_{\max} > \gamma_0$, draw a trade-off curve and select the controller that most adequately fits the design specifications. Otherwise increment k and go back to Step 3.

This design method is illustrated by the following simple numerical example.

5.1. Example

In this example we consider the following system matrices

$$A = \begin{bmatrix} 0 & 1 \\ 2 & 1 \end{bmatrix}, \quad B_0 = B_1 = \begin{bmatrix} 0 \\ 0 \end{bmatrix}, \quad B_2 = \begin{bmatrix} 0 \\ 1 \end{bmatrix},$$
$$C_0 = [-1 \quad 0], \quad C_1 = [0 \quad 0], \quad C_2 = [-1 \quad 1],$$
$$D_0 = 1, \quad D_{12} = 1, \quad D_{21} = 1$$

Notice that $w = w_0 = w_1$ and we will be able to compare the optimal H_2/H_∞ controller with the central controller and with that obtained from the minimization of an upper bound to the objective function [3, 13]. For this data the value of $\gamma_{\min} = 12.01$ and γ_0 was set to 12.02. Four designs were tried, namely, with the central H_∞ controller labeled **C**, the suboptimal minimization of an upper bound to the H_2 norm labeled **S** and the application of the proposed algorithm for the two possible output feedback controller parametrizations discussed in Section 4.3.2. For this simple example, both parametrizations provided virtually the same result in terms of the minimized H_2 and, for this reason, they are uniquely labeled as **O**. The trade-off curves can be seen in Figure 1. Also plotted are the lower bounds provided by $\gamma_{\min}$ and $\|T(z_0, w; s)\|_2$ calculated with the nominal H_2 optimal controller.

For low values of γ, we observe that the controller **S** provides poor performance, even worse than that of the central controller **C**. For large values of γ the situation is reversed, which can be easily understood, since the minimized upper bound becomes closer to the

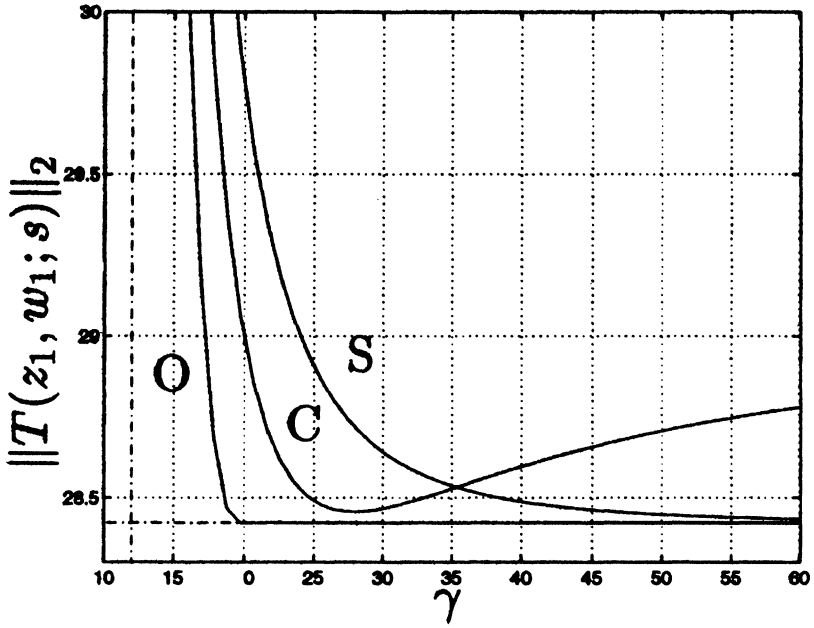

FIGURE 1 Trade-off curves.

actual H_2 norm and the suboptimal controller tends to the optimal H_2 controller. Denoting by $\gamma_2 = 19.7$ the $\|T(z_1, w; s)\|_\infty$ calculated with the H_2 optimal controller, we see that the controller **O** has the best performance and indeed matchs the H_2 minimal norm. In fact, as Figure 2 suggests, controller **O** approximately meets the global optimality conditions since $\|T(z_1, w; s)\|_\infty$ is close to γ for $\gamma \leq \gamma_2$ and approximately equal to γ_2 for larger values of γ. Also notice that for $\gamma < \gamma_2$, $\|T(z_1, w; s)\|_\infty$ is always larger than the H_∞ norms calculated with the controllers **C** and **S**, which explains its better H_2 performance.

These curves were drawn taking 30 equaly spaced points between γ_0 and $\gamma_{\max} = 60$. Since the proposed algorithm converges to local optimal solutions to the mixed H_2/H_∞ problem, the degree of optimality of each obtained solution may critically depend on the initialization. In this way different discretization strategies over γ may change the shape of the trade-off curve, How this fact could be explored will be the subject of further investigations.

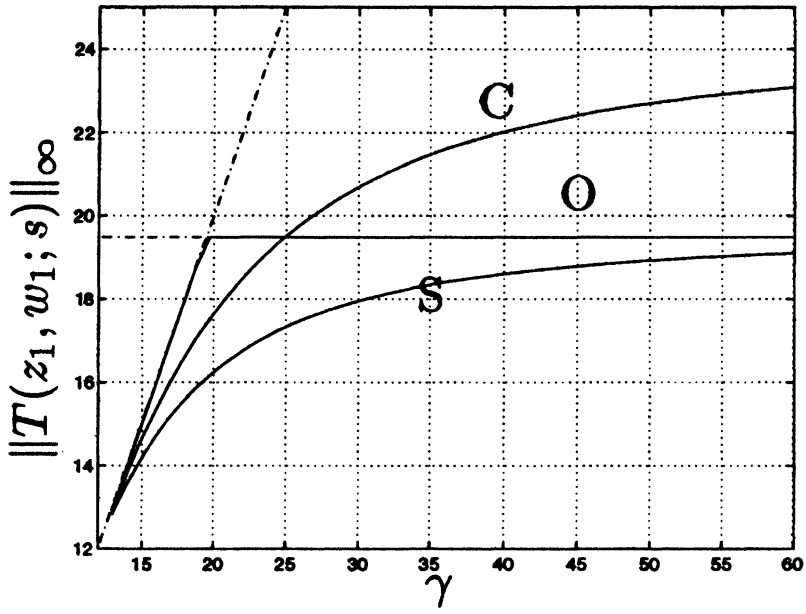

FIGURE 2 H_∞ norms.

6. FLEXIBLE STRUCTURE DESIGNS

In this section we perform some numerical experiments that illustrate the features of the design methods proposed in this paper applied to typical flexible structure models. Although the design problems are based on theoretical models, we believe that the specifications we draw and the several experiments we conduct might illustrate how many of the difficulties faced in actual flexible structures designs can be dealt with the proposed strategies.

The flexible structures [15, 16] we consider have infinite dimensional linear models in the form (1), (2) with natural frequencies ω_i, $i=1,\ldots,\infty$, to be determined as the solution of given algebraic equations. If the structure is excited by m impulsive input forces applied at the points p_j, $j=1,\ldots,m$ each row of the input matrix B is calculated as

$$B_i = [\phi_i(p_1)\cdots\phi_i(p_j)\cdots\phi_i(p_m)], \quad i=1,\ldots,\infty$$

where $\phi_i(p)$, $i=1,\ldots,\infty$ are functions to be determined. Those functions also let us evaluate the output displacements and velocities by

$$z(p,t)=\sum_{i=1}^{\infty}\phi_i(p)x_i(t), \quad \dot{z}(p,t)=\sum_{i=1}^{\infty}\phi_i(p)\dot{x}_i(t)$$

which define the infinite dimensional matrices E and F. In the sequel we introduce two particular models we are going to deal with [17].

Model I The first model is an homogeneous variable cross section rod with one free end as illustrated in Figure 3. In this figure both perturbation (u_p) and control (u_c) forces are assumed to act axially and z represents the axial displacement. Calling M_0 the linear mass density, E the modulus of elasticity and A_0 the maximum cross section area it is possible to determine time undamped linear model parameters in the following way. Defining

$$\kappa=\sqrt{\frac{M_0}{EA_0}}$$

the natural frequencies ω_i, $i=1,\ldots,\infty$ are calculated as the zeros of the algebraic equation

$$\mathcal{J}_0(\kappa l\omega)=0$$

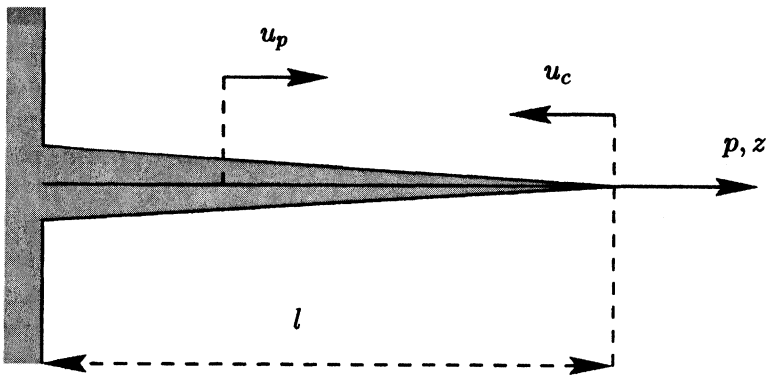

FIGURE 3 Model I: variable cross section rod.

where $\mathcal{J}_n(\cdot)$ denotes the Bessel function of order n, while the entries of function $\phi(p)$ are determined by

$$\phi_i(p) = \frac{1}{\sqrt{M_0 l}} \frac{\mathcal{J}_0(\kappa(l-p)\omega_i)}{\mathcal{J}_1(\kappa l \omega_i)}, \quad i = 1, \ldots, \infty$$

We consider that the control input u_c is placed at $p = l$ and that the perturbation input u_p is placed at $p = 0.63l$. Furthermore we assume that matrix B is partitioned in the form

$$B = [B_c \; B_p]$$

where the submatrices B_c and B_p account for u_c and u_p, respectively. The control structure is collocated, that means, the measured output y is also taken at $p = l$. We assume that both displacement and velocity at $p = l$ are measured. In the following experiments the constants are set to $M_0 = 1\,\text{kg/m}$, $EA_0 = 1\,\text{N}$ and $l = 10\,\text{m}$.

Model II The second model is an homogeneous constant cross section flexible beam simply supported at both ends as illustrated in Figure 4. On the contrary of the variable section rod the perturbation (u_p) and control (u_c) forces act transversally and z represents the transversal displacement. Calling M_0 the linear mass density, E the modulus of elasticity and I the area moment of inertia it is possible to determine the undamped linear model parameters where the natural

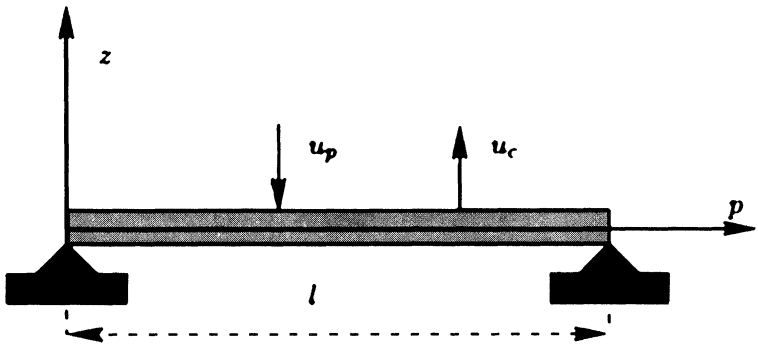

FIGURE 4 Model II: constant cross section beam.

frequencies ω_i, $i=1,\ldots,\infty$ are given as

$$\omega_i = (\pi_i)^2\sqrt{\frac{EI}{M_0 l^4}}, \quad i=1,\ldots,\infty$$

and the entries of function $\phi(p)$ are determined by

$$\phi_i(p) = \sin\left(\frac{p\pi i}{l}\right)\sqrt{\frac{2}{M_0 l}}, \quad i=1,\ldots,\infty$$

For this second structure the control input u_c is placed at $p=3.5l$ and the perturbation input u_p is set at $p=0.65l$. Once more we partition matrix B in the form

$$B = [B_c \; B_p]$$

in order to account for both inputs u_c and u_p. The control structure is also collocated and y contains both displacement and velocity measurements. In the following experiments $M_0=1\,\text{kg/m}$, $EI=1\,\text{N}$ and $l=10\,\text{m}$.

6.1. Reference Models

For practical purposes we truncate the given infinite dimensional models taking only the first $N=12$ modes and consider the corresponding state space models in the form (5), (6), with 24 states, as our *reference* models. Damping is added by taking $\xi=0.01$ for all modes. With respect to the matrices in the generalized plants (13)–(16), we define the following augmented perturbation input

$$w_0 = \begin{bmatrix} u_p \\ u_n \end{bmatrix}$$

where u_n is a measurement noise, and define matrices B_0 and D_{20} as

$$B_0 = [B_p \quad 0], \quad D_{20} = [0 \quad I]$$

Furthermore the control input is taken as $u=u_c$ so that $B_2=B_c$. The open loop impulsive displacement response of both structures with respect to the perturbation inputs u_p are shown in Figures 5 and 6 as solid lines. In the same figures, also as solid lines, we find the corresponding Bode diagrams.

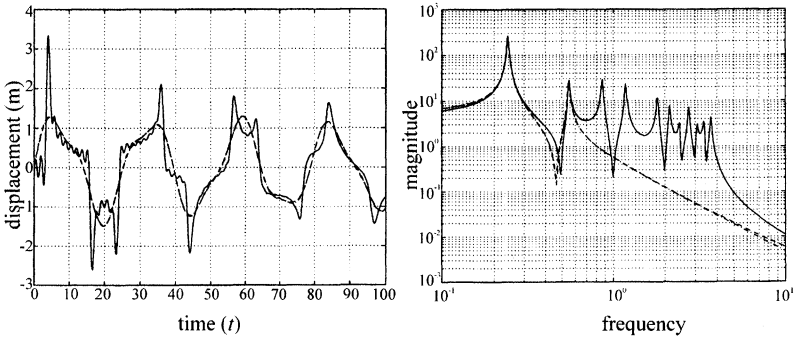

FIGURE 5 Model I: open loop impulsive responses and Bode diagrams.

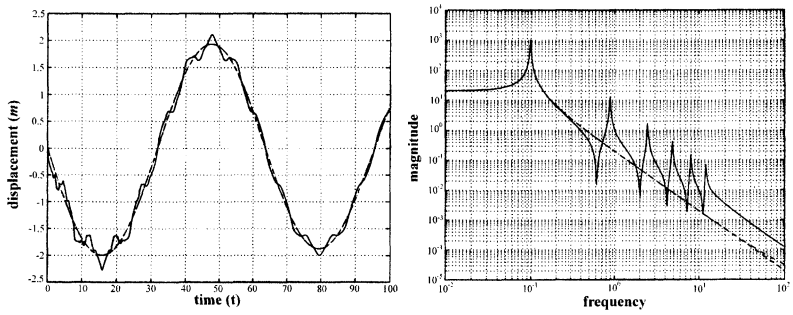

FIGURE 6 Model II: open loop impulsive responses and Bode diagrams.

6.2. Reduced Order Design

The design of reduced order output feedback controllers is still an open problem in the literature. Most design procedures provide controllers which have the same order as that of the generalized plant to be controlled. In the control of flexible structure this point may become critical due to the generally high order of the considered plants. In this scenario, possible strategies are the design of full order controllers followed by some possible controller reduction or the design of controllers for a reduced plant. In the first case, the main problem is how to reduce the controller without losing the properties associated to the full order design. In the second case, the question to be answered is how we can ensure that the controller designed for the

reduced plant will be effective with respect to the original high order plant. In this section we take the second way, trying to design reduced order controllers that we hope will perform well face to the high order system by introducing some robustness considerations in the design. So, given a high order plant, a reduced order design procedure could be outlined as follows: (a) reduce the high order plant by some order reduction procedure, (b) design a controller for the reduced order plant trying to minimize a given performance index while keeping robustness in some sense, (c) check the design with respect to the original high order plant.

In this paper, we perform Step (a) using the balanced-truncation procedure [8]. This procedure consists in applying to a system of order n in the form (5), (6) a special similarity transformation followed by truncating the state vector to order n_r. We choose the order of the reduced dynamic n_r by looking at the index [7]

$$\rho(k) = \left(\frac{\sum_{i=k+1}^{n} \sigma_i^4}{\sum_{i=1}^{n} \sigma_i^4} \right)^{1/2}$$

where σ_i are the singular values of the product of the controlability and observability grammians associated to (5), (6). We truncate the system to order n_r when $\rho(n_r)$ becomes sufficiently less than 1.

Then the reduced order design problem is taken in the mixed H_2/H_∞ control problem context. Robustness is considered with respect to the uncertainty model (12) while performance in the H_2 setup is measured by the cost outpimt z_0 defined by

$$C_0 = \begin{bmatrix} I \\ 0 \end{bmatrix}, \quad D_0 = \begin{bmatrix} 0 \\ 1 \end{bmatrix}$$

with respect to the augmented perturbation input w_0. Notice that the input associated to robustness (w_1) is quite different from the perturbation input (w_0), which fits time design procedures proposed in the previous sections in a very suitable manner. The particular results for the two considered structures follow.

Model I With respect to the order reduction procedure [8], as can be seen in Figure 7, it is not easy to choose the order of the reduced model. Since there is no abrupt reduction in the value of $\rho(k)$ that may

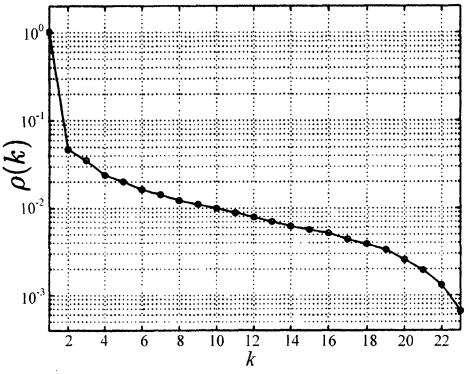

FIGURE 7 Model I: order reduction.

suggest internal dominancy of some reduced order model it is difficult to find a single value below which $\rho(k)$ can be considered *sufficiently* less than 1. Almost arbitrarily we take $n_r = 4$. The impulse response of the obtained reduced plant (dashed line) can be seen and compared with the full order response (solid line) in Figure 5.

Robustness is introduced according to the model (12) with $\alpha = 10$. In this way we are mainly considering uncertainty in the dynamic rather than in the input and output matrices. This is quite natural in this setup since the main source of errors in the system description comes with the truncation of some modes performed by the reduction procedure. So, following the steps given in Section 5 we determined $\gamma_{\min} = 74.81$ and set $\gamma_0 = 74.89$. The minimal H_2 norm controller, *i.e.*, the controller which minimizes $\|T(z_0, w_0; s)\|_2$ without taking care of $\|T(z_1, w_1; s)\|_\infty$ was calculated, providing the closed loop norms $\|T(z_1, w_1; s)\|_\infty = 557.3$ and $\|T(z_0, w_0; s)\|_2 = 3.28$. It is interesting to notice that although this controller is unable to stabilize the given reference model, the value of the associated H_2 and H_∞ norms still provides guidelines for the whole design process. Then, we have run the algorithm and plotted the design trade-off curve seen in Figure 8 for values of γ between γ_0 and $\gamma_{\max} = 8\gamma_0 \approx 600$. In this figure the curves have been obtained using 8×10 equally spaced points and the solid line corresponds to the closed loop H_2 norm with the local optimal mixed H_2/H_∞ controller while the dashed line shows the same function calculated with the central controller. Notice that for large

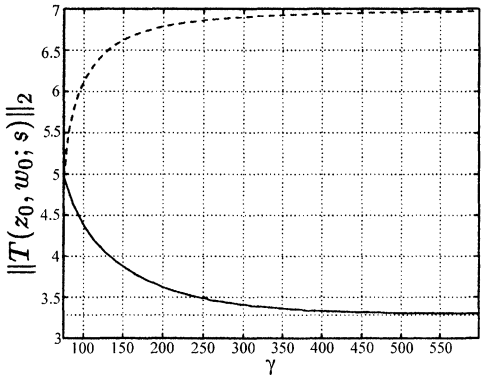

FIGURE 8 Model I: trade-off curve.

values of γ the value of $\|T(z_0, w_0; s)\|_2$ approaches that of the optimal H_2 controller, represented in the figure as a dotted lower bound line. In this sense, as we can see, once again the design procedure was able to provide H_2 cost that are near optimal. Since w_0 is not equal to w_1 we may not compare this design with the suboptimal controller discussed in the first example. Also remarkable is the fact that, in the considered interval, the value of $\|T(z_0, w_0; s)\|_2$ associated with the central H_∞ controller never decreases, which suggests that, on the contrary of what happens in the first example, relaxing γ without minimizing the H_2 norm will not produce controllers better than the minimal central H_∞ controller.

Keeping in mind that the main objective is to stabilize the reference model, we might select a value of γ which is sufficiently far from $\gamma_{\max}$, since we know that the optimal H_2 is not stabilizing. As a compromise solution we chose $\gamma^* = 271.5 \approx 0.5 \times 557.3$. As discussed in Section 2 we expect that the controller will be able to support unstructured perturbations in the reduced model such that

$$\|\Delta_1\|_\infty < 3.68 \times 10^{-3}, \quad \|\Delta_i\|_\infty < 0.37 \times 10^{-3}, \quad i = 2, 3$$

For our purposes, although this level of robustness seems to be very small, it is more than enough and we have been able to obtain reduced order controllers which stabilize the reference model with values of γ up to 7 times γ_0. So, with this choice of γ^* we are indeed providing some extra robustness with respect to the reference model.

Furthermore, in terms of performance $\|T(z_0, w_0; s)\|_2$ is just 5% larger than the optimal destabilizing H_2 norm. Closed loop controller performance may be evaluated by looking at Figure 9, where the responses of the controlled reference model to an impulse at u_p are plotted for the local optimal mixed H_2/H_∞ controller (solid) and for the minimal central H_∞ controller (dashed). This closed loop behavior seems to be compatible with controllers obtained by other design approaches [9].

Continuing to illustrate the performance of the obtained controller, although we have used the impulsive input as a valuable analysis and design tool, it is also interesting to probe the controller performance face to more realistic disturbance inputs which, on the contrary of the impulse, typically may present a more attenuated spectral distribution at high frequencies. Once the design procedure was based on a reduced order model which does not accurately represents the high frequency behavior of the reference model (see Fig. 5), we may expect that the obtained controller performs even better when excited by low frequency inputs. To check this, for both controllers considered before, we simulate the closed loop response of the reference model with respect to the test inputs $A(A_d, T)$ (solid line) and $B(A_d, T)$ (dashed line) depicted in Figure 10. The simulations for the optimal mixed H_2/H_∞ controller (solid) and for the optimal H_∞ controller can be found in Figures 11 and 12.

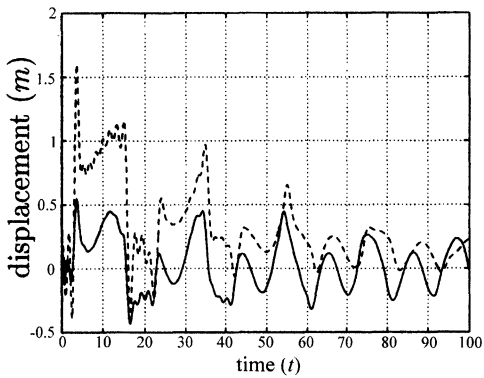

FIGURE 9 Model I: closed loop impulsive response.

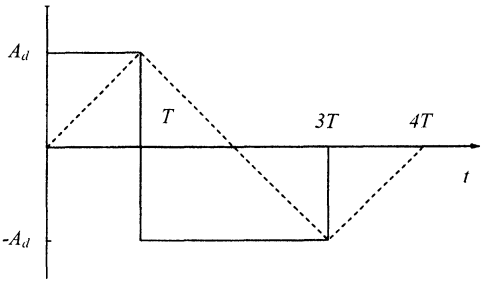

FIGURE 10 Test disturbances $A(A_d, T)$ and $B(A_d, T)$.

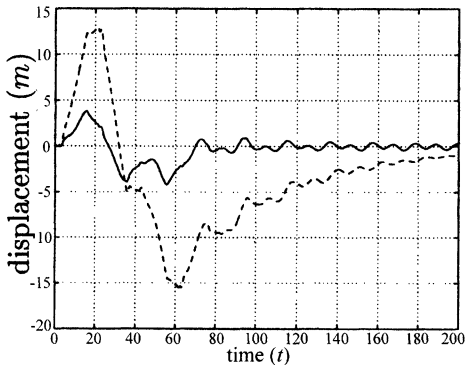

FIGURE 11 Model I: closed loop response to disturbance $A(1, 20)$.

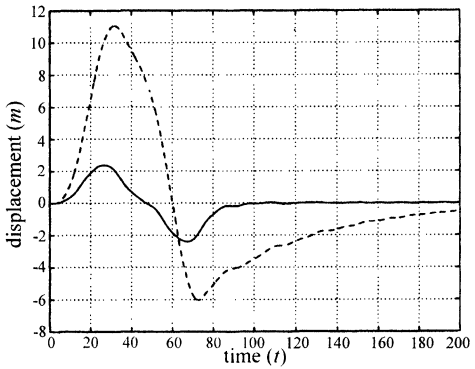

FIGURE 12 Model I: closed loop response to disturbance $B(1, 20)$.

Model II Looking at $\rho(k)$ plotted for the reference model II in Figure 13, we notice that in this case it is much easier to choose the order to be considered by the reduction procedure [8]. The abrupt reduction in the value of $\rho(k)$ at $k=2$ suggests the presence of a dominant system of order two[2] so we take $n_r=2$. The impulsive response of the obtained reduced plant (dashed line) can be compared with the full order response (solid line) in Figure 6.

For the reasons discussed in the previous example we consider the uncertainty model (12) with $\alpha=20$. Then we calculate $\gamma_{\min}=56.27$ and set $\gamma_0=56.33$. In this case, however, as a consequence of the more accurate description provided by the reduced order model, the minimal H_2 norm controller is able to stabilize the reference model and provides the closed loop norms $\|T(z_1, w_1; s)\|_\infty=164.8$ and $\|T(z_0, w_0; s)\|_2=3.17$. So, we took 3×10 equally spaced points between γ_0 and $\gamma_{\max}=3\gamma_0\approx 170$ and plotted the trade-off curves seen in Figure 14. Once again the solid line corresponds to the closed loop H_2 norm calculated with the local optimal mixed H_2/H_∞ controller while the dashed line shows the same function for the minimal central H_∞ controller. In this case, as we know that the optimal H_2 controller stabilizes the reference model, we may be less conservative and choose $\gamma^*=116.4\approx 0.7\times 164.8$. As for the model I, unstructured

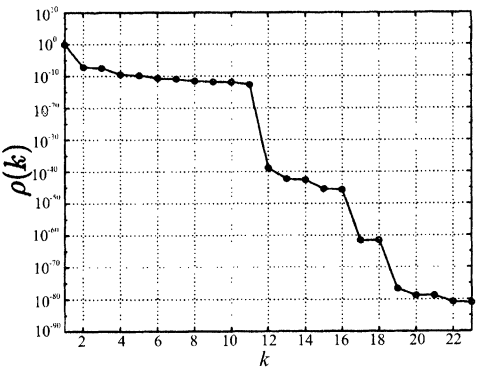

FIGURE 13 Model II: order reduction.

[2]Almost evident in the impulsive response and Bode graphs (Fig. 6).

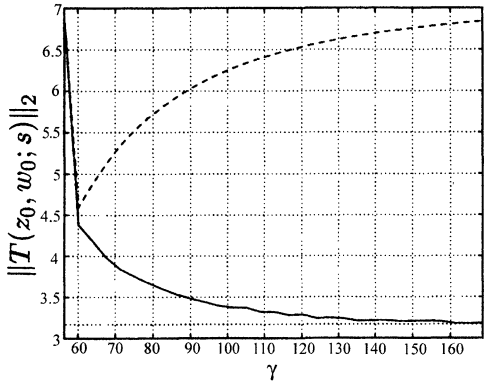

FIGURE 14 Model II: trade-off curve.

perturbation bounds can be easily calculated and the performance level happens to be just 3% larger than the optimal H_2 norm. The responses of the reference model to an impulse at u_p are depicted in Figure 15, where the closed loop response with the minimal central H_∞ controller (dashed), with the local optimal mixed H_2/H_∞ controller (solid) and with the optimal H_2 controller (dash-dot) have been plotted. Notice that the impulsive response associated to the optimal H_2 controller presents a lightly undamped high frequency mode that is completely damped by the H_2/H_∞ mixed design. Except for this fact, the response of both controllers is almost identical, and

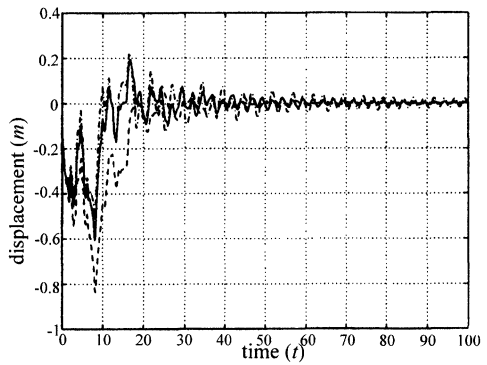

FIGURE 15 Model II: closed loop impulsive response.

much better than the response of the optimal H_∞ controllers. In this sense, we may say that the extra degree of robustness achieved by the mixed design provided adequate closed loop performance associated to an additional high frequency damping not provided by the pure H_2 controller. When working with reduced order models, which typically do not accurately describe high frequency modes, this high frequency damping is a very desirable and welcome property. At last, Figures 16 and 17 show the closed loop responses to the previously introduced test inputs.

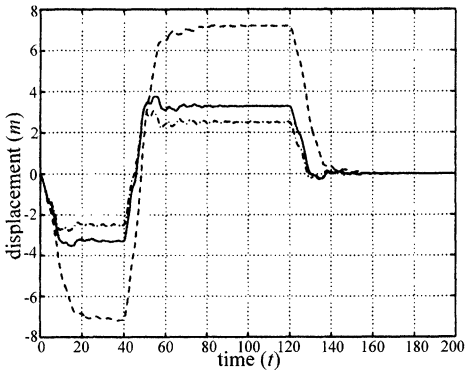

FIGURE 16 Model II: closed loop response to disturbance $A(1, 40)$.

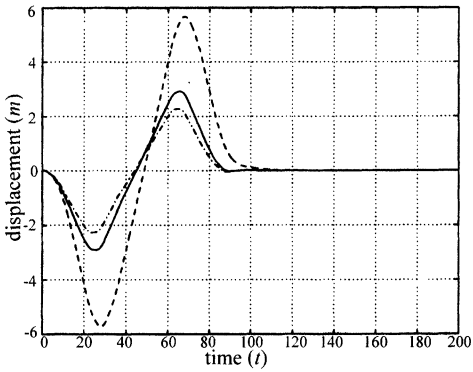

FIGURE 17 Model II: closed loop response to disturbance $B(1, 40)$.

6.3. Truncated Order Design

In order to illustrate the application of the more elaborate uncertainty description (7), (8) we will try to design controllers for low order truncated versions of the introduced infinite dimensional models which are able to stabilize the given reference models. That truncation will simply be performed retaining the first $n_r/2$ modes of the considered flexible structure Models I and II. It is worth noticing that, on the contrary of what we have done in the last section, we do not mean to propose the truncation followed by the determination of a mixed H_2/H_∞ controller as an alternative to the design of low order controller, since the truncation procedure may provide a very rough and imprecise description of complex flexible structure dynamics. As we will show, for the very simple models we are dealing with, truncation does happen to provide an accurate description of the high order system behavior, and, with the main intention of illustrating the interesting features of the mixed H_2/H_∞ controller design we are proposing, will be considered along with the uncertainty models (7), (8). Nevertheless, the reader should be aware that the main application of the mixed H_2/H_∞ design with this uncertainty models (7), (8) is the project of controllers based on imprecise linear models given in the form (1), (2).

With respect to this uncertainty models (7), (8), its main advantage compared with (12), is the reduction of the degree of conservativeness associated to the H_∞ constraint. From the developments in Section 2, models (7), (8) is built in order to take into account the particular state space representation of flexible structure models.

In the following examples, we consider H_2 performance as we did in the reduced order design, defining the measured cost output z_0, with

$$C_0 = \begin{bmatrix} I \\ 0 \end{bmatrix}, \quad D_0 = \begin{bmatrix} 0 \\ I \end{bmatrix}$$

The other inputs and outputs are also kept as in the reduced order design.

Model I For this first model, in order to get a truncated model with the same order as that of the reduced order design, we consider only the first 2 modes of the system, which provide a state space representation with order $n_r = 4$. The impulse response and the Bode

diagram of the obtained truncated plant (dash-dot) can be seen and compared with the full order (solid) and the reduced order (dashed) plots in Figure 5. Notice that, as stated before, in this simple example the reduced and the truncated plants almost coincide, which may not be true for more complex flexible structure models.

In the uncertainty models (7), (8) we have also set $\alpha = 10$. With these settings, we have found $\gamma_{\min} = 43.78$ and set $\gamma_0 = 43.82$. Surprisingly enough, the minimal H_2 norm controller is able to stabilize the reference model providing the closed loop norms $\|T(z_1, w_1; s)\|_\infty = 386$ and $\|T(z_0, w_0; s)\|_2 = 1.47$. Taking 9×10 equaly spaced points between γ_0 and $\gamma_{\max} = 9\gamma_0 \approx 390$ we plotted the trade-off curves seen in Figure 18 for the optimal mixed H_2/H_∞ controller (solid) and the minimal central H_∞ controller (dashed). As a compromise solution we have chosen $\gamma^* = 78.87 \approx 0.2 \times 386$. Notice that this value of γ^* is about 5 times smaller than the value of $\|T(z_1, w_1; s)\|_\infty = 386$ associated with the optimal H_2 controller and that the optimal mixed H_2/H_∞ cost $\|T(z_0, w_0; s)\|_\infty = 1.81$ is about 23% larger than the optimal H_2 cost. So, we may expect that this controller will have a very poor performance when compared with the controller obtained in the reduced order design, which seems to be much more close to the optimal H_2 performance. However, comparing the simulations in Figures 19–21 with those in Figures 9, 11 and 12 we notice that the closed loop controller performances are very similar. We believe that

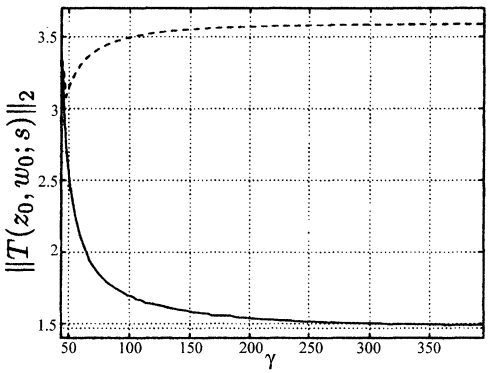

FIGURE 18 Model I: trade-off curve.

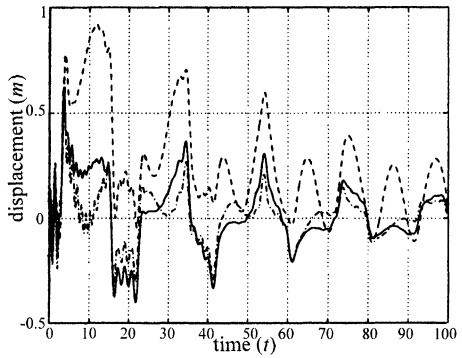

FIGURE 19 Model I: closed loop impulsive response.

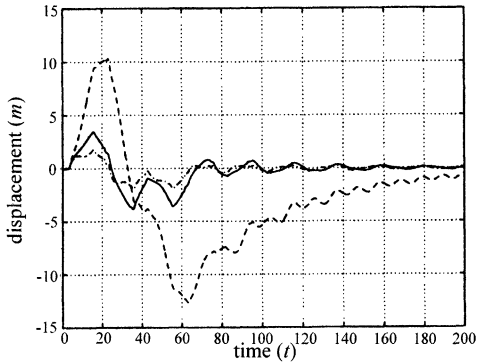

FIGURE 20 Model I: closed loop response to disturbance $A(1, 20)$.

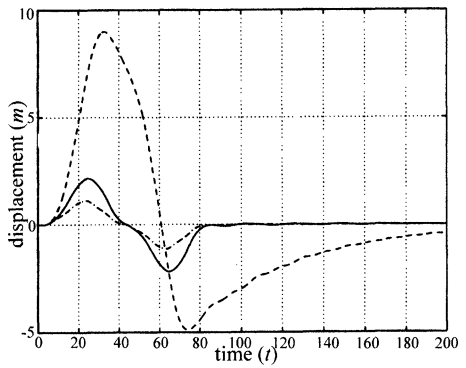

FIGURE 21 Model I: closed loop response to disturbance $B(1, 20)$.

this fact can be explained due to the differences in the uncertainty models (7), (8) and (12). Once the uncertainty models (7), (8) *fits* best the actual dynamic errors than model (12), the conservativeness introduced by the requirement of an extra robustness level is such that the closed loop performance does not seem to be significantly affected. In that sense it is interesting to notice that the responses calculated with the minimal central H_∞ controllers are slightly better in the truncated design than in the reduced design.

Model II For model II we have kept only the first mode of the original model which provides a state space model with $n_r = 2$ states. As in the previous example, the reduced and the truncated plants almost coincide, which can be seen in the impulsive response and Bode diagrams in Figure 6 for the truncated (dash-dot), full order (solid) and the reduced order (dashed) systems.

The uncertainty model is taken as (7), (8) with $\alpha = 20$. We have calculated $\gamma_{\min} = 55.4$ and set $\gamma_0 = 55.5$. The minimal H_2 norm controller provides the closed loop norms $\| T(z_1, w_1; s) \|_\infty = 124$ and $\| T(z_0, w_0; s) \|_2 = 1.75$ and stabilizes the reference model. The trade-off curve in Figure 22 is plotted taking 3×10 equally spaced points between γ_0 and $\gamma_{\max} = 3\gamma_0 \approx 170$, where the solid line is drawn for the local optimal mixed H_2/H_∞ controller and the dashed line for the central H_∞ controller. We have chosen the value of $\gamma^* = 103.8 \approx 0.8 \times 124$ which gives an H_2 performance just 1% larger

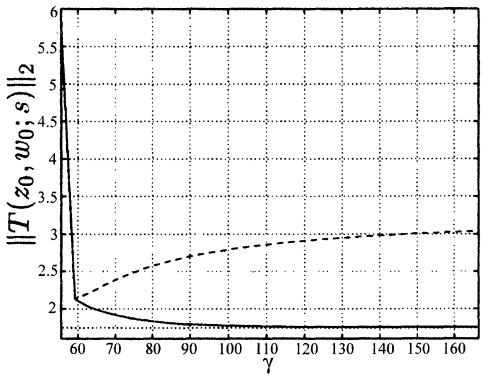

FIGURE 22 Model II: trade-off curve.

than the optimal H_2 performance. The closed loop time simulations can be found in Figures 23–25 for the minimal central H_∞ controller (dashed), the local optimal mixed H_2/H_∞ controller (solid) and the optimal H_2 controller (dash-dot). As in the reduced order design the performance of the mixed design is very close to the optimal H_2 performance with extra damping of the high frequencies, a fact that becomes very clear in Figure 23.

6.4. Comments

Some comments about the solved problems are now in order. First, we see that the performance of the algorithm and the associated design

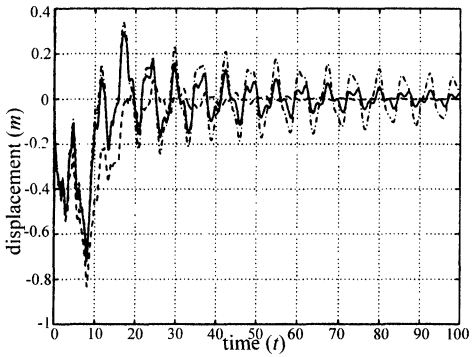

FIGURE 23 Model II: closed loop impulsive response.

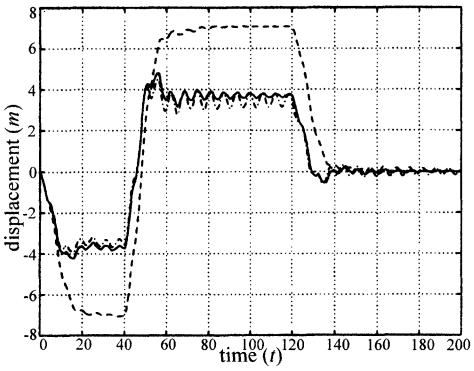

FIGURE 24 Model II: closed loop response to disturbance $A(1, 40)$.

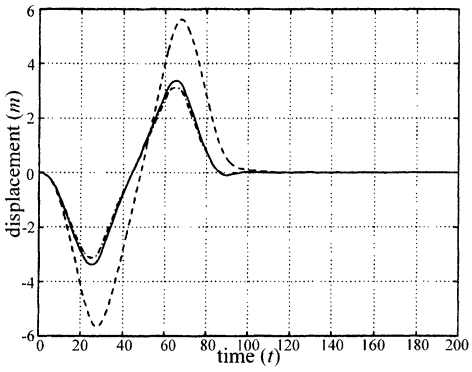

FIGURE 25 Model II: closed loop response to disturbance $B(1, 40)$.

procedure seem to be very satisfactory. In all the examples we can notice that the value of the H_2 norm for large values of γ indeed matches the optimal H_2 norm (see Figs. 1, 8, 14, 18 and 22). Furthermore, the trade-off curves turned out to be a very useful tool, helping in the selection of the desired levels of robustness/performance to be provided by the mixed controller.

A second remark is that the design of reduced order controllers based on models pre-processed by the balanced-truncation algorithm may be very interesting if associated with the uncertainty model (12). Even for plants for which it is difficult to chose an appropriate reduction order (as Model I), the introduction of robustness considerations in a mixed H_2/H_∞ context seems to provide an adequate framework for achieving low order controllers with good performance.

Finally, notice that the only free parameter of the uncertainty models introduced in Section 2 that have been changed in the examples was α, which is increased in order to emphasize the importance of the imprecise description of the dynamics. None of the matrix scalings have been used.

7. CONCLUSION

In this paper an unstructured H_∞ uncertainty model is introduced to cope with the design of full order linear dynamic output feedback

robust controllers for flexible structures. This model is built taking into account perturbations around a given nominal linear model in modal coordinates. The same uncertainty model is further extended to cope with less structured reduced order system models.

Robust performance is considered in the mixed H_2/H_∞ setup for a six port generalized plant. The controller is parametrized such that the resultant problem is formulated as the minimization of a non-convex but differentiable objective function subject to a convex constraint. A numerical algorithm which is able to find a local optimal solution to this problem is introduced.

A controller design procedure is developed providing a trade-off curve that allows to choose a controller that best fits the robustness/performance requirements. A simple numerical example illustrates the method and provides a comparison with other procedures, namely the suboptimal minimization of an upper bound to the H_2 norm and the central H_∞ controller, in which the controller introduced in this paper always achieves the best performance.

The procedure is applied to two different flexible structure theoretical models providing satisfactory results, which are verified by several simulations.

References

[1] Geromel, J. C., Bernussou, J. and de Oliveira, M. C. (1999). "H_2 norm optimization with constrained dynamic output feedback controllers: decentralized and reliable control", *IEEE Transactions on Automatic Control*, **44**(7), 1449–1454.

[2] de Oliveira, M. C. and Geromel, J. C. (2000). "Design of decentralized dynamic output feedback controllers *via* a separation principle", *International Journal of Control*, **73**(5), 371–381.

[3] Colaneri, P., Geromel, J. C. and Locatelli, A., *Control Theory and Design: An RH_2–RH_∞ viewpoint*, San Diego, CA: Academic Press, 1997.

[4] Boulet, B., Francis, B. A., Hugues, P. C. and Hong, T. (1997). "Uncertainty modeling and experiments in H_∞ control of large flexible space structures", *IEEE Transactions on Control Systems Technology*, **5**(5), 504–519.

[5] Balas, G. J. and Doyle, J. C., "Robustness and performance tradeoffs in control design for flexible structures", In: *Proceedings of the American Control Conference*, 1991.

[6] Smith, R. S., Chu, C. C. and Fanson, J. L. (1994). "The design of H_∞ controllers for an experimental noncollocated flexible structure problem", *IEEE Transactions on Control Systems Technology*, **2**, 101–109.

[7] Moore, B. C. (1981). "Principal components analysis in linear systems: controllability, observability and model reduction", *IEEE Transactions on Automatic Control*, **26**(1).

[8] Safonov, M. G. and Chiang, R. Y. (1989). "A schur method for balanced-truncation model reduction", *IEEE Transactions on Automatic Control*, **34**(7).
[9] de Souza, C. C. (1994). Optimal output feedback control of flexible structures, *Ph.D. Thesis*, UNICAMP.
[10] Luenberger, D. G., *Introduction to Linear and Nonlinear Programming*, Addison Wesley, 1973.
[11] Nesterov, Y. E. and Nemirovskii, A. (1994). *Interior Point Polynomial Methods in Convex Programming*, Philadelphia, PA: SIAM.
[12] de Oliveira, M. C. and Geromel, J. C., "Interior point methods and LMI", *Proceedings of the XI Brazilian Conference on Automation*, Sao Paulo, Brazil, 1996, pp. 353–358.
[13] Baeyens, E. and Khargonekar, P. P., "Some examples in mixed H_2/H_∞ control", In: *Proceedings of the American Control Conference* (Baltimore, Maryland), 1994.
[14] Scherer, C., "Mixed H_2/H_∞ control for linear parametrically varying systems", In: *Proceedings of the IEEE Conference on Decision and Control*, pp. 3182–3187.
[15] Meirovitch, L., *Elements of Vibrational Analysis*, New York, NY: McGraw Hill, 1986.
[16] Meirovitch, L., *Analytical Methods in Vibrations*, New York, NY: The MacMillan Co., 1967.
[17] Meirovitch, L., Barah, H. and Oz, H. (1983). "A comparison of control techniques for large flexible systems", *Journal of Guidance*, **6**.

APPENDIX A: GRADIENT CALCULATION

In this appendix we calculate the gradient of function (20)

$$f(L,X) = \text{trace}\left[(C_0 + D_0LX^{-1})P(C_0 + D_0LX^{-1})'\right]$$

Recalling that P is the unique positive definite solution to

$$(A + B_2K)P + P(A + B_2K)' + B_0B_0' = 0$$

where $K = LX^{-1}$ one may calculate the gradient of $f(L, X)$ by taking the Lagrangean function

$$\begin{aligned}\mathcal{L} = &\text{trace}[(C_0 + D_0K)P(C_0 + D_0K)']+\\ &+\text{trace}[\Lambda\{(A + B_2K)P + P(A + B_2K)' + B_0B_0'\}]\end{aligned}$$

where $\Lambda = \Lambda'$. Imposing

$$\frac{\partial\mathcal{L}}{\partial P} = (A + B_2K)'\Lambda + \Lambda(A + B_2K) + (C_0 + D_0K)'(C_0 + D_0K) = 0$$

it follows that

$$\frac{df}{dK} = \frac{\partial \mathcal{L}}{\partial K} = 2[B_2'\Lambda + D_0'(C_0 + D_0K)]P$$

Now, since $\Delta K = \Delta L X^{-1} - K\Delta X X^{-1}$ an remembering that $X = X'$

$$\frac{\partial f}{\partial L} = \frac{df}{dK}X^{-1}, \quad \frac{\partial f}{\partial X} = \frac{1}{2}\left(- K'\frac{df}{dK}X^{-1} - X^{-1}\frac{df'}{dK}K\right).$$